Microporous and Mesoporous Materials 290 (2019) 109642

Contents lists available at ScienceDirect

Microporous and Mesoporous Materials

journal homepage: www.elsevier.com/locate/micromeso

Functionalized MIL-53(Fe) as efficient adsorbents for removal of tetracycline antibiotics from aqueous solution

Jun Yu[a,b,1], Weiping Xiong[a,b,1], Xin Li[a,b,1], Zhaohui Yang[a,b,*], Jiao Cao[a,b], Meiying Jia[a,b], Rui Xu[a,b], Yanru Zhang[a,b]

[a] College of Environmental Science and Engineering, Hunan University, Changsha, 410082, PR China
[b] Key Laboratory of Environmental Biology and Pollution Control (Hunan University), Ministry of Education, Changsha, 410082, PR China

ARTICLE INFO

Keywords:
MIL-53(Fe)
Functionalized
Adsorption
Tetracycline

ABSTRACT

Recently, metal-organic frameworks with high porosity have drawn extensive attention in environment remediation. Herein, a variety of porous metal-organic frameworks were synthesized, including MIL-53(Fe), NH_2-MIL-53(Fe), NO_2-MIL-53(Fe) and Br-MIL-53(Fe), to adsorb tetracycline (TCN) from aqueous solution. Results showed that the functionalized MIL-53(Fe) exhibited higher adsorption performance than the pristine MIL-53(Fe). Among MIL-53(Fe) series, Br-MIL-53(Fe) had the highest maximum adsorption capacity of 309.6 mg g^{-1}. Effects of initial pH values, co-existed ions and humic acid on the adsorption performance of functionalized MIL-53(Fe) were investigated. The adsorption kinetics fitted well with pseudo-second order model and the adsorption isotherms matched Langmuir model, which suggested that the adsorption process was dominant by chemisorption and the adsorption surface was homogenous. Additionally, adsorption thermodynamics showed that the adsorption process of TCN on MIL-53(Fe) series were spontaneous and endothermic. More importantly, the functionalized MIL-53(Fe) demonstrated excellent recyclability and the detailed adsorption mechanism was discussed. Therefore, this work provided a strategy for fabrication of efficient MOFs-based adsorbent for antibiotic-containing wastewater treatment.

1. Introduction

Antibiotics, especially tetracycline antibiotics, are widely utilized in healthcare, animal husbandry and fish farming, due to their low cost, obvious effect and wide antimicrobial spectrum [1]. However, the abuse of antibiotics has caused serious environmental issues for their persistence, biological accumulation and long-distance migration, which have posed a latent threat to human health [2,3]. It was reported that the concentration of antibiotics in raw domestic sewage was in the range of 100 ng L^{-1}-6 mg L^{-1}, while the antibiotics concentration was even detected in the range of 100-500 mg L^{-1} in pharmaceutical and hospital wastewater [4]. As a consequence, an economical and effective method was needed for the remediation of antibiotic pollutants in water environments.

To date, various methods have been intensively investigated to eliminate antibiotics in aquatic environment, including electrochemical method [5], advanced oxidation processes (AOPs) [6], biological method [7], anaerobic digestion [8] and membranes separation [9]. However, these strategies have some deficiencies, which severely restricts their extensive utilization in practical applications. For instance, electrochemical method and AOPs may releases by-products which can cause secondary pollution. Some antibiotic residues are unable to be effectively removed by traditional biological methods owing to their antibacterial properties [10]. Additionally, membrane separation process suffers from membrane fouling because of the accumulation of contaminants on membrane surface [11]. Fortunately, adsorption shows superiority in wastewater treatment for its low operation cost, none secondary pollution and high removal efficiency [12]. Recently, various porous materials have been reported as promising adsorbents, such as activated carbons [13], multiwall carbon nanotubes [14] and graphene oxide [15]. However, few of these materials show high efficiency, selectivity and stability for antibiotics adsorption. Therefore, it is imperative to develop adsorbents with excellent properties [16].

Metal-organic frameworks (MOFs) are a relatively emerging kind of porous materials, have caused widespread concerns and achieved enormous development in the last decade. MOFs are constructed by self-assemble of metal cations/clusters and organic ligands [17,18]. MOFs

* Corresponding author. College of Environmental Science and Engineering, Hunan University, Changsha, Hunan, 410082, China.
E-mail address: yzh@hnu.edu.cn (Z. Yang).
[1] These authors contribute equally to this article.

https://doi.org/10.1016/j.micromeso.2019.109642
Received 6 March 2019; Received in revised form 12 July 2019; Accepted 2 August 2019
Available online 03 August 2019
1387-1811/

with high specific surface area, high porosity and structural diversity as well as adjustable pore size/shape, have demonstrated diverse potential applications in pollutants removal, chemical sensing, catalysis and gas storage [19,20]. Recently, adsorption using MOFs is not only one of the most widely investigated applications but also becoming one of the most prospective applications. So far, MOFs have been reported much for adsorptive removal hazardous substances from aqueous solutions. For example, Yang et al. utilized Ce(III)-doped UiO-66 to adsorbed organic dyes from aqueous solution. The adsorption capacity of Ce (III)-doped UIO-66 for methylene blue was 490% higher than the pristine UiO-66 because of the increased specific surface area [21]. And Yue et al. obtained hierarchical porous Zn-MOF-74 with a specific surface area of 759 $m^2 g^{-1}$ by a template-free strategy which showed excellent adsorption potential [22]. Abazari et al. reported various nanostructured MOF with high amoxicillin antibiotics adsorption capacity of 486.4 mg g^{-1} [23]. The other reports of antibiotics removal from aqueous solution including tetracycline on MIL-101(Cr) [24], ciprofloxacin on ZIF-8 [25], sulfonamide antibiotics on HKUST-1 [26] and so on. Therefore, it is necessary to synthesis MOF-based materials with excellent adsorption performance. The MIL-53(M) series is a typical class of MOFs with the advantages of flexible structure, stable chemical properties and breathing feature stability [27]. Furthermore, the high-valence metal ion center of Fe^{3+} with the most commonly used carboxylate-type ligands can be easily applied to synthesized water stable MOFs [28].

In general, regulating the properties of MOFs by grafting with specific functional groups is an effective strategy to improve the adsorption performance of adsorbents. Besides, the strategy of grafting can be simply achieved by importing functional groups on organic ligands [29]. Hence, in this work, the -NH_2, -NO_2 and -Br groups were introduced in MIL-53(Fe) by one-step solvothermal method. Scanning electron microscope (SEM), X-ray power diffractometer (XRD), Fourier transform infrared spectrum (FTIR) and Brunauer-Emmett-Teller (BET) were utilized to characterized the physical and chemical properties of as-obtained MIL-53(Fe)-based adsorbents. The adsorption performance of functionalized MIL-53(Fe) for TCN adsorption was investigated and the possible adsorption mechanisms were proposed. The effects of initial pH values, co-existed ions and humic acid on adsorptive removal of TCN were analyzed. Moreover, the reusability of adsorbents was studied. Excellent adsorption performance of functionalized MIL-53(Fe) provided a new sight on tetracycline removal.

2. Experimental section

2.1. Chemicals

Reagents used in this experiment included N, N-dimethylformamide (DMF, 99.5%), Iron(III) chloride hexahydrate ($FeCl_3{\cdot}6H_2O$, 99%), tetracycline (TCN), ethanol (99.5%), terephthalic acid (H_2BDC, 99%), 2-aminoterephthalic acid (2-NH_2-H_2BDC, 99%), nitro-terephthalic acid (2-NO_2-H_2BDC, 99%) and 2-bronoterephthalic acid (2-Br-H_2BDC, 99%) which were all purchased from Sinopharm Chemical Reagent Co., Ltd (Shanghai, China). All of the above chemicals were analytical reagent grade and used without purification.

2.2. Synthesis of adsorbents

MIL-53(Fe) was prepared according to our previously reported literature [14]. In a typical solvothermal method, $FeCl_3{\cdot}6H_2O$ (0.674 g) and 1, 4-H_2BDC (0.415 g) were added into a beaker which containing 56 mL DMF solution. Subsequently, stirring for 1 h at room temperature and then poured the as-prepared solution into a 100 mL Teflon-lined stainless-steel autoclave and kept at 170 °C for 24 h. After cooling down to room temperature, the solids were washed with DMF and ethanol and collected by centrifugation. Finally, the yellow products were vacuum dried under 100 °C for several hours.

NH_2-MIL-53(Fe) was obtained by one-step solvothermal method according to the literature with some modifications [30]. Typically, $FeCl_3{\cdot}6H_2O$ (0.674 g), 2-NH_2-H_2BDC (0.452 g) and 56 mL DMF were mixed in a beaker with continuous stirring for 1 h at room temperature. Next, poured the clarified solution into a 100 mL Teflon-lined stainless-steel autoclave and heated at 170 °C for 24 h. Subsequently, after cooling the obtained NH_2-MIL-53(Fe) solids were washed with DMF and ethanol for several times and separated by centrifugation. At last, the brown products were dried in vacuum at 100 °C for several hours. As the same methods, the NO_2-MIL-53(Fe) was synthesized by 0.674 g of $FeCl_3{\cdot}6H_2O$ and 0.525 g of 2-NO_2-H_2BDC, the Br-MIL-53(Fe) was synthesized by 0.674 g of $FeCl_3{\cdot}6H_2O$ and 0.610 g of 2-Br-H_2BDC.

2.3. Characterization methods

Scanning electron microscope (SEM) was performed on a Carl Zeiss (EVO-MA10, Germany) system. X-ray power diffraction (XRD) patterns were measured by a D8 Bruker diffractometer with Cu Kα X-ray source. Fourier transform infrared spectroscopy (FTIR) measurements were recorded on a Nicolet 5700 Spectrometer (Nicolet, USA). The N_2 adsorption-desorption isotherms were performed on a Quantachrome (USA) analyzer and the adsorption parameters of samples were obtained by Brunauer-Emmett-Teller method. The zeta potentials of adsorbents at different initial pH values were measured by Zeta-sizer Nano-ZS (Malvern, UK).

2.4. Adsorption experiments

The whole adsorption experiments were performed in the form of batch adsorption. The 1000 mg L^{-1} stock solution of TCN was obtained by dissolving 1 g of TCN powders into ultra-pure water. The different concentration of TCN solution used in adsorption experiments were prepared by diluting the stock solution. The initial pH value was 7.0 which was adjusted by adding NaOH or H_2SO_4 (0.01–0.1 M). All adsorption experiments were performed in a constant temperature water bath shaking table with a constant vibration speed of 300 rpm stirring for 24 h. Ultraviolet visible spectrophotometer was used to measurement TCN concentrations at 357 nm. The calibration curves of TCN were measured at a concentration of 5–60 mg L^{-1}. The adsorption capacity of adsorbents were calculated according to the following formula:

$$q_e = \frac{(C_0 - C_e)V}{m} \quad (1)$$

In equation (1), C_0 (mg L^{-1}) is the initial concentrations of TCN and C_e (mg L^{-1}) is the equilibrium concentrations. m (g) is the mass of adsorbents and V (L) is the volume of TCN solutions.

The adsorption kinetics experiments were studied by adding 10 mg adsorbents to 50 mL of 20 mg L^{-1} TCN solutions. Residual TCN concentrations were measured at a predetermined time interval (5 min–24 h). The adsorption isotherms of were performed at a condition of TCN concentrations 5–200 mg L^{-1} with an initial pH 7.0 at 298 K. The thermodynamic properties of MIL-53(Fe) series were performed at 298, 308 and 318 K, respectively. The effect of initial pH was studied at 298 K. The initial pH values were in the range of 3–10 which was obtained by adding negligible volume of 0.01–0.1 M NaOH or H_2SO_4 solution. Subsequently, the experiment influencing factors of co-existed ions were investigated. This involved adding NaCl or $CaCl_2$ to 20 mg L^{-1} TCN solutions which contained 10 mg adsorbents and the concentrations of NaCl or $CaCl_2$ were in the range of 0–9 g L^{-1}. Furthermore, the effect of HA concentration on adsorption were studied. In this adsorption experiment, TCN concentration was confirmed at 20 mg L^{-1} and the concentration of HA were between 0 and 40 mg L^{-1}. Finally, the regeneration experiments after adsorption were explored using ethyl alcohol as the eluent of TCN.

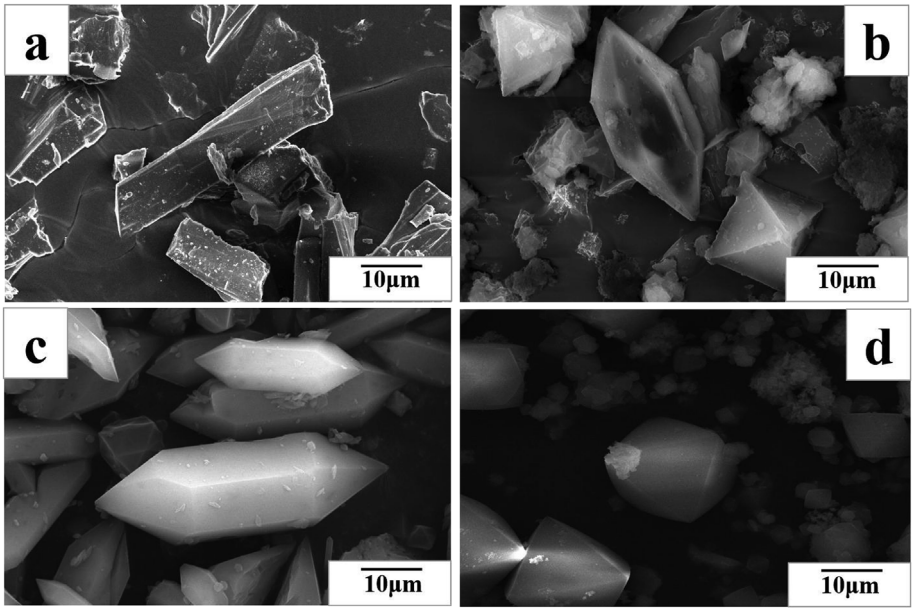

Fig. 1. The SEM images of MIL-53(Fe) (a) NH_2-MIL-53(Fe) (b) NO_2-MIL-53(Fe) (c) and Br-MIL-53(Fe) (d).

3. Results and discussion

3.1. Characterization of the MIL-53(Fe) series

The surface morphology of the as-prepared samples was characterized by SEM (Fig. 1). Fig. 1a showed that the MIL-53(Fe) particles exhibited a rod-like crystallites with an average width of 10 μm. However, the surface morphology of functionalized MIL-53(Fe) was changed obviously. As shown in Fig. 1b and c, NH_2-MIL-53(Fe) and NO_2-MIL-53(Fe) displayed a typical bipyramidal hexagonal prism structure with sharp edges and had a smooth surface. And Br-MIL-53(Fe) showed a cubic octahedron structure which surface was smooth. The introduction of diverse branched groups on the organic ligands had effect on the morphology of MIL-53(Fe). Besides, the SEM images showed that the MIL-53(Fe) samples grafting with various group had different size. NH_2-MIL-53(Fe) and NO_2-MIL-53(Fe) revealed a more regular shape and uniform size. While Br-MIL-53(Fe) had a smaller average diameter of 10 μm than NH_2-MIL-53(Fe) and NO_2-MIL-53(Fe).

The FTIR spectra measurements were investigated to revealed the connection of characteristic functional groups between functionalized MIL-53(Fe) and MIL-53(Fe). As shown in Fig. 2, there were characteristic peaks at 538 cm^{-1}, 750 cm^{-1}, 1390 cm^{-1}, 1540 cm^{-1} and 1650 cm^{-1} in the MIL-53 (Fe) infrared spectrogram, which were corresponded to the Fe-O stretching vibration, C-H, C-O, C-O and C = O, respectively [31]. For NH_2-MIL-53(Fe), the characteristic peak at 3794 cm^{-1} was attributed to the asymmetrical vibrations of amine moieties [32]. Besides, the characteristic peaks of NH_2-MIL-53(Fe) at 1246 cm^{-1} and 1689 cm^{-1}, which were characteristic C-N stretching vibration and N-H bending vibration of aromatic amines in the lower frequency region. As displayed in NO_2-MIL-53(Fe), the spectrum of the NO_2-MIL-53(Fe) exhibited a band at 1556 cm^{-1} which corresponded to a asymmetric vibrations of -NO_2 [33]. The FTIR spectrum of Br-MIL-53(Fe) was quite similar to the MIL-53(Fe). In the FTIR curve of Br-MIL-53(Fe), there was no typical C-Br stretching vibration bands around 550 cm^{-1}, which was partially covered by the stretching vibration of Fe-O [34].

The crystalline phase of MIL-53-(Fe), NH_2-MIL-53(Fe), NO_2-MIL-53(Fe) and Br-MIL-53(Fe) were obtained by X-ray diffraction (XRD) analysis (Fig. 3). The XRD pattern of pristine MIL-53(Fe) was in perfect fitted with the previous reported which indicated the successful synthesis of MIL-53(Fe) [35]. After modification by grafting different

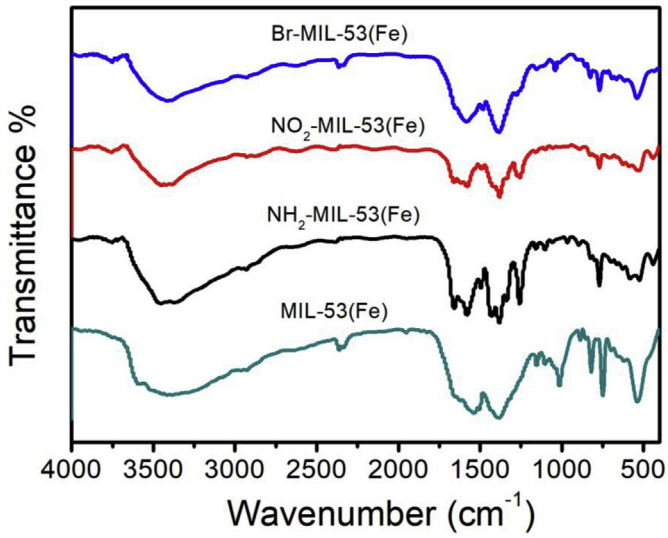

Fig. 2. The FTIR spectra of MIL-53(Fe) series.

functional groups, all diffraction peaks of functionalized MIL-53(Fe) were in accordance with the MIL-53(Fe) pattern, which suggested that the introduction of ligand substituents had no effect on the framework structure of MIL-53(Fe).

The adsorption parameters of the as-prepared adsorbents were obtained by BET method and the result was illustrated in Fig. 4 and Table 1. Fig. 4 indicated that all the MIL-53(Fe) series had a type H3 hysteresis and all the curves corresponded to the typical type IV isotherms. The result could be due to the volume filling theory of mesoporous [36]. As shown in Table 1 showed, after grafting with functional groups, the pore size of functionalized MIL-53(Fe) was smaller than pristine MIL-53(Fe). Additionally, the BET surface area increased in the order of NO_2-MIL-53(Fe) < Br-MIL-53(Fe) < MIL-53(Fe) < NH_2-MIL-53(Fe). This conditions probably because of the additional volume of introduced functional group and the partial destruction of the MIL-53(Fe) series structures during the modifications under harsh conditions [37].

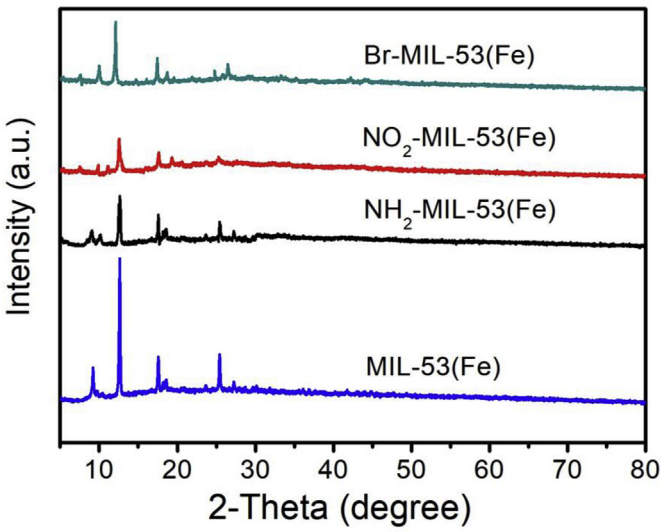

Fig. 3. The XRD patterns of MIL-53(Fe) series.

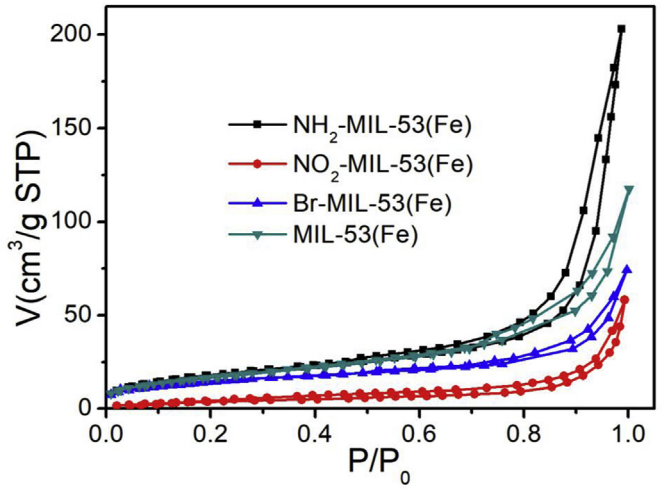

Fig. 4. N_2 adsorption-desorption isotherms of MIL-53(Fe) series.

3.2. Adsorption kinetics and adsorption isotherms

The effect of different initial contact time and different initial concentrations were investigated and the result was illustrated in Fig. S1 and Fig. S2. Details of the results and discussions were contained in the Supplementary Information. The adsorption data of MIL-53(Fe) series were fitted well with pseudo-second order model (Fig. 5). It suggested that the rate limiting step in the adsorption process might be the chemisorption [38]. The adsorption of TCN onto MIL-53(Fe) series fitted well with Langmuir isotherm models (Fig. S2 and Table 2), which confirmed that the surface adsorption sites on adsorbents were homogeneous distribution and the adsorption of TCN on MIL-53(Fe) series might occurred in the monolayer mode [24].

3.3. Adsorption thermodynamics

The effect of different temperature was assessed for adsorption experiments. As shown in Fig. S4, with the increase of temperature, the adsorption rate of MIL-53(Fe) series increased obviously but the temperature had a slight effect on the equilibrium adsorption capacity of MIL-53(Fe) series. To better evaluated the effect of temperature, the thermodynamic parameters of enthalpy change (ΔH), Gibbs free energy (ΔG) and entropy change (ΔS) could be calculated according to the following equations [39].

$$\ln C_e = \frac{\Delta H}{RT} + K \tag{2}$$

$$\Delta G = -RT\ln K_\alpha \tag{3}$$

$$K_\alpha = 10^6 K_L \tag{4}$$

$$\Delta S = \frac{\Delta H - \Delta G}{T} \tag{5}$$

In equations (2)–(5), R is the gas constant (8.314 J mol^{-1} K^{-1}); T (K) is thermodynamic temperature; K_α is the thermodynamic equilibrium constant and K_L (L mg^{-1}) is Langmuir equilibrium constant.

The slope of fitted curves (Fig. S5) contrasted with ΔH/R and the thermodynamics parameters were obtained in Table 3. As shown in Table 3, the ΔG values of all adsorbents were negative which illustrated the TCN adsorption over MIL-53(Fe) series were spontaneous and thermodynamically favorable. Furthermore, with the increased of temperature, the values of ΔG decreased which confirmed that the adsorption process at higher temperature might promoted TCN adsorption onto adsorbents. The ΔH values of MIL-53(Fe), NH_2-MIL-53(Fe), NO_2-MIL-53(Fe) and Br-MIL-53(Fe) were 49.6, 11.6, 3.7, 9.4 kJ mol^{-1}, respectively. It could be due to the TCN adsorption over MIL-53(Fe) series were a physicochemical adsorption process [40]. Moreover, the positive ΔH values implied TCN adsorption were a typical endothermic process, which were consistent with adsorption thermodynamics experiments. The positive ΔS values demonstrated that an increased randomness occurred at the solid-liquid interface. In a word, the adsorption process was an endothermic and spontaneous process.

3.4. Effect of pH and co-existed ions

The effect of pH values on TCN adsorption of functionalized MIL-53(Fe) were shown in Fig. 6a. All of the functionalized MIL-53(Fe) revealed a decent adsorption performance for TCN. The maximum adsorption capacity of NH_2-MIL-53(Fe) and NO_2-MIL-53(Fe) at pH 7.0 were 73.2 mg L^{-1} and 87.4 mg L^{-1}, respectively, while the maximum adsorption capacity of Br-MIL-53(Fe) at pH 9.0 was 95.1 mg L^{-1}. In addition, the zeta potential of functionalized MIL-53(Fe) were measured to further analyzed the trend of observed results. As shown in Fig. 6b, the neutral charge of NH_2-MIL-53(Fe), NO_2-MIL-53(Fe) and Br-MIL-53(Fe) were at pH 8.1, 7.5 and 6.5, respectively. The dissociation constants (pK_a) of TCN were 3.32, 7.78 and 9.58, illustrating TCN at

Table 1
Surface area, pore size and pore volume parameters of MIL-53(Fe) series.

Samples	MIL-53(Fe)	NH_2-MIL-53(Fe)	NO_2-MIL-53(Fe)	Br-MIL-53(Fe)
Surface area[a] (m^2 g^{-1})	52.18	65.64	30.01	39.75
Pore size[b](nm)	8.81	3.80	4.85	4.07
V_t[c] (cm^3 g^{-1})	0.115	0.314	0.243	0.107

[a] Measured using N_2 adsorption with the Brunauer-Emmett-Teller (BET) method.
[b] Pore size in diameter calculated by the desorption data using Barrett-Joyner-Halenda (BJH) method.
[c] Total pore volume determined at P/P_0 = 0.99.

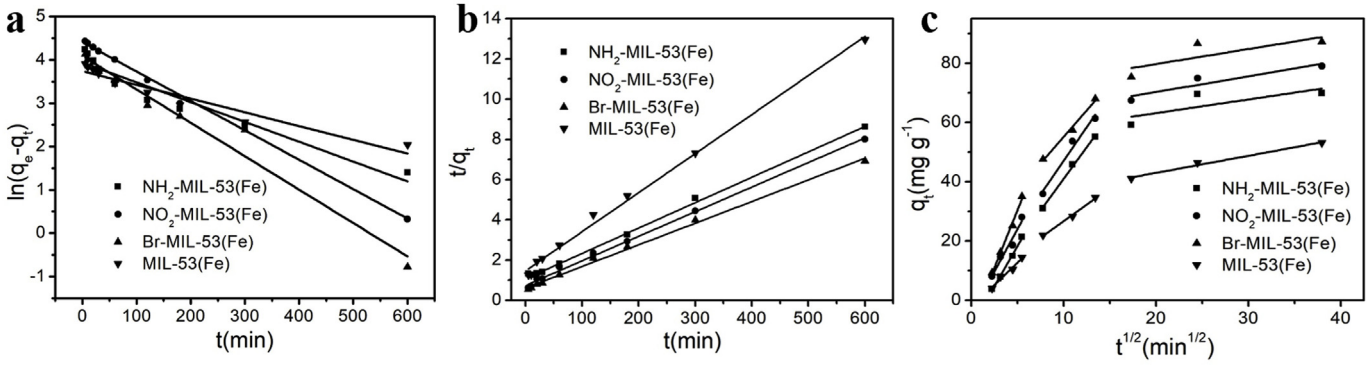

Fig. 5. The pseudo-first order model (a) pseudo-second order model (b) and intra-particle diffusion model for TCN adsorption.

pH < 3.32 was positive charge, at 3.32 < pH < 7.78 was neutral charge and at pH > 7.78 was negative charge. Therefore, there would be no electrostatic interaction at 3.32 < pH < 7.78, repulsive interactions would be observed at pH > 8.1 for TCN adsorption over NH_2-MIL-53(Fe) and NO_2-MIL-53(Fe), attractive interaction would be observed at pH > 8.1 for TCN adsorption over Br-MIL-53(Fe). However, the tendencies shown in Fig. 6 were quite different from that expected. Besides, the removal process still had a certain amount of adsorption for TCN at pH 3.0–10.0, which indicated that the mechanism of TCN adsorption process was not dominated by electrostatic interaction. It could be attributed that TCN adsorption process was mainly occurred by the π-π interaction, because of the presence of benzene rings on TCN and MIL-53(Fe) series [41].

Actually, the composition of domestic and industrial effluents are complex, the inorganic ions usually coexist with the organic pollutants and salts. The effect of co-existed ions on functionalized MIL-53(Fe) adsorption performance were shown in Fig. 7. When NaCl or $CaCl_2$ was added in the TCN solution, the adsorption of TCN on functionalized MIL-53(Fe) were obviously inhibited. On one hand, the overall trend of adding NaCl or $CaCl_2$ to the solution were similar, with the increased of ionic strength, the adsorption capacity decreased. This phenomenon might be caused by the addition ions could compete the adsorptive sites of functionalized MIL-53(Fe) with TCN molecules. On the other hand, the inhibitory effect of $CaCl_2$ adsorption in TCN was greater than NaCl, which could be interpreted as that Ca^{2+} had more charge at the same concentration than Na^+, resulting in a stronger competitive adsorption and TCN.

3.5. Effect of humic acid

Humic acid (HA) is ubiquitous in natural water environment systems and is mainly obtained by the microbial decomposition and transformation of the dead plant matters [42]. Fig. 8 showed the TCN adsorption capacity of functionalized MIL-53(Fe) with different HA adding. When HA was added, the adsorption capacity of functionalized MIL-53(Fe) decreased. It illustrated that the presence of HA inhibited TCN adsorption onto MOFs. In general, the interactions between HA and MOFs surface were complicated because the existence of sp2 and sp3 components in MIL-53(Fe) series [43]. There were abundant functional groups in HA molecules, such as phenolic hydroxyls and carboxylates. Those functional groups caused the zeta potential of HA at pH > 1.5 was negative. For this reason, HA could interact with TCN molecules. Accordingly, the competitive adsorption between TCN-HA compounds and HA-MOFs in aqueous solution inhibited TCN adsorption onto MOFs [44]. Furthermore, the inhibitory effect could be due to that HA occupied some of the surface adsorption sites through strong π-π interactions [45].

Table 3
The thermodynamic parameters of TCN adsorption on MIL-53(Fe) series.

Samples	T(K)	ΔH (KJ mol^{-1})	ΔS (KJ mol^{-1} K^{-1})	ΔG (KJ mol^{-1})
MIL-53(Fe)	298	49.6	0.245	−23.6
	308			−24.4
	318			−25.1
NH_2-MIL-53(Fe)	298	11.6	0.116	−23.0
	308			−23.8
	318			−24.6
NO_2-MIL-53(Fe)	298	3.7	0.0902	−23.1
	308			−23.9
	318			−24.7
Br-MIL-53(Fe)	298	9.4	0.107	−22.5
	308			−23.2
	318			−24.0

3.6. The possible adsorption mechanism

To obtain deeper understanding of TCN adsorption over MIL-53(Fe) series, the possible mechanisms of adsorption were investigated. The

Table 2
Langmuir, Freundlich and Temkin isotherms parameters for TCN adsorption on MOFs.

Isotherm models	Parameters	Samples			
		MIL-53(Fe)	NH_2-MIL-53(Fe)	NO_2-MIL-53(Fe)	Br-MIL-53(Fe)
Langmuir	$q_{m,exp}$ (mg g^{-1})	248.3	265.3	269.8	307.4
	$q_{m,cal}$ (mg g^{-1})	247.7	271.9	272.6	309.6
	K_L (L g^{-1})	0.0135	0.0109	0.00868	0.0113
	R^2	0.995	0.999	0.994	0.995
Freundlich	K_F [(L $mg^{-1})^{1/n}$ mg g^{-1}]	11.6	15.8	18.5	18.2
	1/n	0.594	0.544	0.519	0.549
	R^2	0.936	0.945	0.926	0.870
Temkin	K_T (L mg^{-1})	0.174	0.207	0.199	0.192
	b (J mol^{-1} g mg^{-1})	37.8	37.2	35.2	30.5
	R^2	0.923	0.935	0.967	0.957

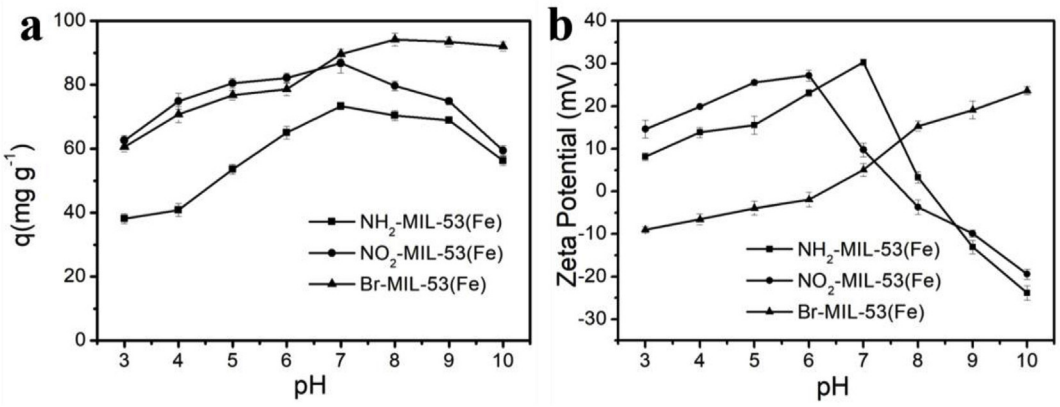

Fig. 6. The effect of pH for TCN adsorption (a) and zeta potential of functionalized MIL-53(Fe). Adsorption conditions: adsorbent loading = 0.2 g L^{-1}; initial TCN concentration = 20 mg L^{-1}; temperature = 298 K. Error bars represent the standard deviation of triplicate samples.

size of tetracycline molecular was 0.5 × 2 nm or so. The pore size of MIL-53(Fe), NH_2-MIL-53(Fe), NO_2-MIL-53(Fe), Br-MIL-53(Fe) were 8.81, 3.80, 4.85, 4.07 nm, respectively. The pore size of MOFs particles was larger than TCN molecules which was conducive to the effective entry of TCN into MOFs. Since the adsorption could happened inside the MOFs. In addition, the pore size of functionalized MOF particles were larger than TCN molecules marginally, which was helpful for suppress the shedding of TCN that had been adsorbed on MOFs [46]. As discussed in BET analysis, the surface area and pore size/volume of MIL-53(Fe) were 52.18 $m^2 g^{-1}$, 8.81 nm and 0.115 $cm^3 g^{-1}$, respectively. However, compared with the pristine MIL-53(Fe), the surface area and pore size/volume of functionalized MIL-53(Fe) inconsistent with the increase of adsorption capacity. Therefore, the TCN adsorption process was not concerned with the physical properties of adsorbents which indirectly indicated that the TCN adsorption process was not dominated by physisorption. The TCN adsorption onto MIL-53(Fe) series were fitted well with pseudo-second order model, proving the adsorption reaction was dominated by chemisorption. Besides, the TCN adsorption TCN adsorption onto MIL-53(Fe) series could be regarded as a monolayer adsorption because the adsorption isotherm obeyed Langmuir isotherms. The TCN adsorption onto MIL-53(Fe) series were mainly occurred by π-π interaction. In addition, the H-receptors functional groups (-NH_2) on NH_2-MIL-53(Fe) and the existence of H-donors groups (-OH) on TCN, which indicated hydrogen bonding interactions might occurred at TCN adsorption onto NH_2-MIL-53(Fe). On the basis of the same π-π interaction, the extra hydrogen bonding interaction caused NH_2-MIL-53(Fe) had higher adsorption capacity than MIL-53(Fe). Besides, the metal centers and Fe-O clusters in MIL-53(Fe) series had Lewis acid properties [47] and TCN molecule was alkalescent because of the existence of amine groups. Moreover, the existence of electron-withdrawing groups (-NO_2, -Br) could provide more strong Lewis acidity. The acid-base interaction between NO_2/Br-MIL-53(Fe)

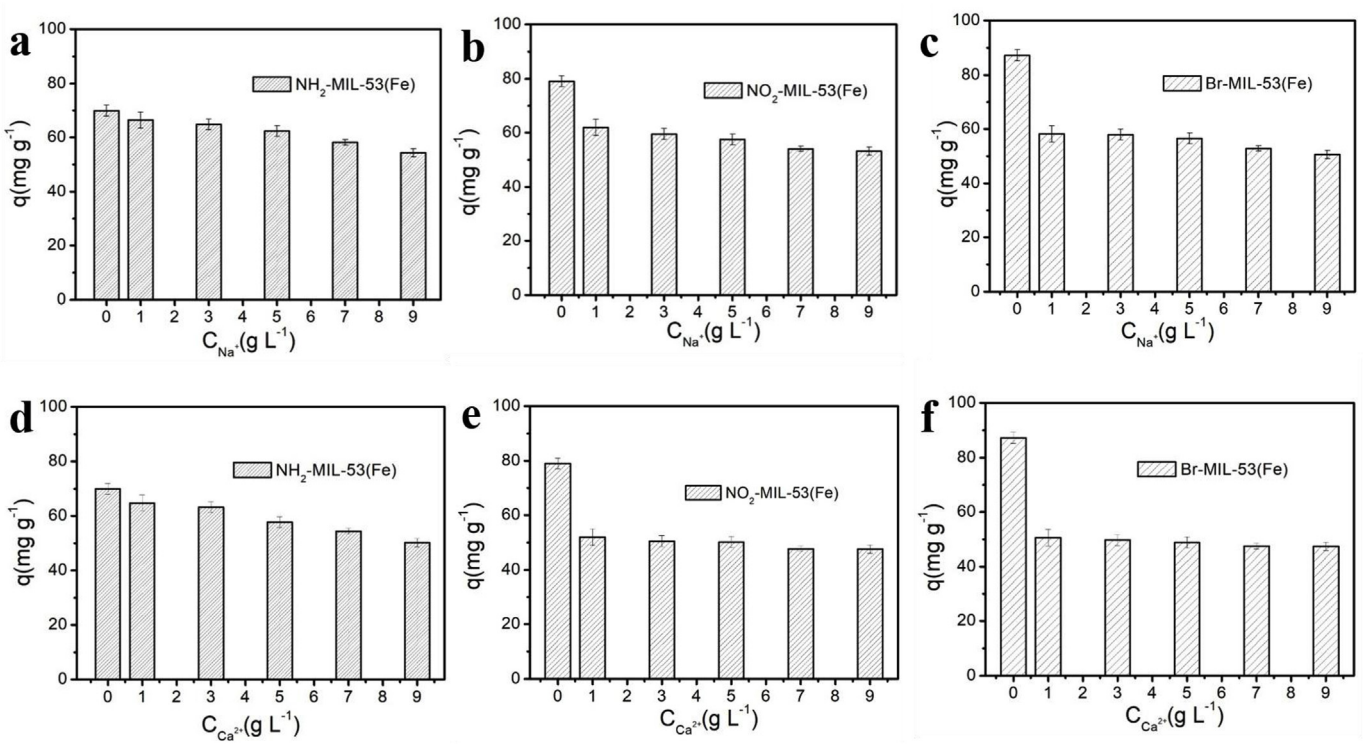

Fig. 7. The effect of NaCl on the adsorption performance of NH2-MIL-53(Fe) (a) NO2-MIL-53(Fe) (b) Br-MIL-53(Fe) (c); the effect of CaCl2 on the adsorption performance of NH2-MIL-53(Fe) (d) NO2-MIL-53(Fe) (e) Br-MIL-53(Fe) (f). Adsorption conditions: adsorbent loading = 0.2 g·L − 1; initial TCN concentration = 20 mg L-1; temperature = 298 K; initial pH = 7. Error bars represent the standard deviation of triplicate samples.

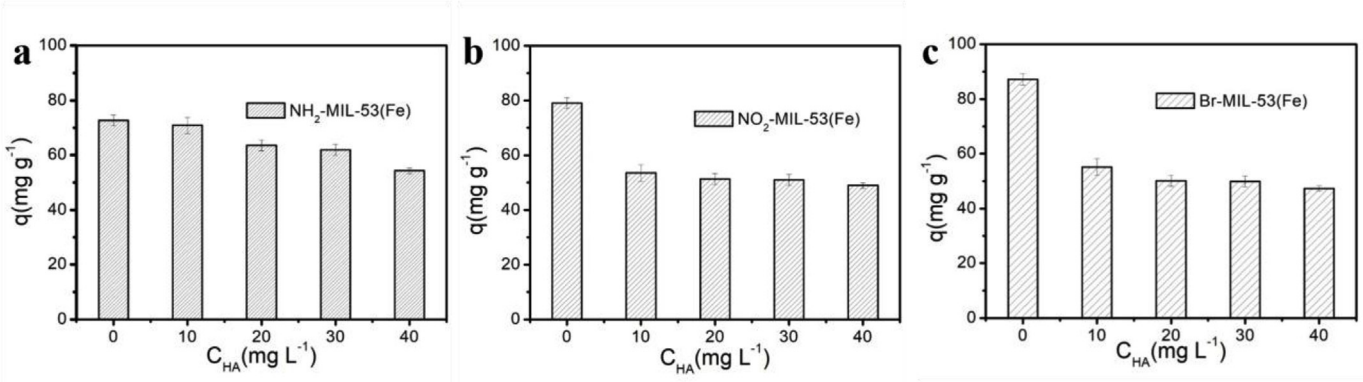

Fig. 8. The effects of humic acid on the adsorption performance of NH_2-MIL-53(Fe) (a) NO_2-MIL-53(Fe) (b) Br-MIL-53(Fe) (c). Adsorption conditions: adsorbent loading = 0.2 g L^{-1}; initial TCN concentration = 20 mg L^{-1}; temperature = 298 K; initial pH = 7. Error bars represent the standard deviation of triplicate samples.

and amine groups of TCN molecules might be a possible mechanism for the chemisorption. Thus, NO_2-MIL-53(Fe) and Br-MIL-53(Fe) had better adsorption performance than MIL-53(Fe). Furthermore, Br-MIL-53(Fe) had more obvious breathing features. The pore of Br-MIL-53(Fe) could change from narrow pore to large pore. With the increasing adsorption amount of Br-MIL-53(Fe) to TCN, the pore size and pore volume of Br-MIL-53(Fe) became higher [48]. The increased pore size and pore volume enables more TCN molecules could be adsorbed into Br-MIL-53(Fe). Therefore, among MOFs series, Br-MIL-53(Fe) had the maximum adsorption capacity. In short, the adsorption of TCN onto the MIL-53(Fe) series was a complicated process. The reason for TCN adsorption on MIL-53(Fe) series should be further investigation.

3.7. Reusability of adsorbents

For practical application, an excellent adsorbent should be reproducible. Therefore, the regeneration experiments of functionalized MIL-53(Fe) were performed by using ethyl alcohol as the eluent of TCN. As shown in Fig. S6, the adsorption capacity of functionalized MIL-53(Fe) could still reach nearly 80% after four adsorption recycles, which indicated excellent reusability of functionalized MIL-53(Fe).

4. Conclusion

In summary, a series of functionalized MIL-53(Fe) were synthesized successfully by a facile solvothermal approach and applied for adsorptive removal of tetracycline antibiotics from aqueous solution. All functionalized MIL-53(Fe) showed a higher adsorption capacity than the pristine MIL-53(Fe). The maximum adsorption capacities of NH_2-MIL-53(Fe), NO_2-MIL-53(Fe) and Br-MIL-53(Fe) for removal TCN can reach 271.8 mg g^{-1}, 272.6 mg g^{-1} and 309.6 mg g^{-1}, respectively. Furthermore, the adsorption kinetic studies indicated that the TCN adsorption process was chemisorption and the results of adsorption isotherms suggested that the adsorbents had a homogenous surface. Besides, the dates of adsorption thermodynamic revealed that the adsorption process were spontaneous and endothermic. More importantly, initial pH, co-existed ion and humic acid had obviously influence on the adsorption properties of functionalized MIL-53(Fe). The adsorption mechanism revealed that the TCN adsorption process was dominated by π-π interaction. Moreover, the presence of NH_2- group provided an extra hydrogen bonding interaction for TCN adsorption on NH_2-MIL-53(Fe). Additional acid-base interaction was occurred between NO_2/Br-MIL-53(Fe) and TCN. Owing to the breathing features of Br-MIL-53(Fe), Br-MIL-53(Fe) had the best adsorption properties among MIL-53(Fe) series. Besides, the functionalized MIL-53(Fe) adsorbents showed excellent reusability which could be reused for four cycles. This study is expected to provide a feasible strategy for the removal of tetracycline antibiotics and broaden the application range of MOFs as adsorbents.

Acknowledgements

The study was financially supported by the National Natural Science Foundation of China (51878258 and 51578223) and the Key Research and Development Program of Hunan Province (2017SK2242).

Appendix A. Supplementary data

Supplementary data to this article can be found online at https://doi.org/10.1016/j.micromeso.2019.109642.

References

[1] S.A. Sassman, L.S. Lee, Sorption of three tetracyclines by several soils: assessing the role of pH and cation exchange, Environ. Sci. Technol. 39 (2005) 7452.
[2] G. Zeng, M. Chen, Z. Zeng, Risks of neonicotinoid pesticides, Science 340 (2013) 1403-1403.
[3] B. Petrie, R. Barden, B. Kasprzyk-Hordern, A review on emerging contaminants in wastewaters and the environment: current knowledge, understudied areas and recommendations for future monitoring, Water Res. 72 (2015) 3–27.
[4] Z.-h. Yang, J. Cao, Y.-p. Chen, X. Li, W.-p. Xiong, Y.-y. Zhou, C.-y. Zhou, R. Xu, Y.-r. Zhang, Mn-doped zirconium metal-organic framework as an effective adsorbent for removal of tetracycline and Cr(VI) from aqueous solution, Microporous Mesoporous Mater. 277 (2019) 277–285.
[5] P. Song, Z. Yang, G. Zeng, X. Yang, H. Xu, L. Wang, R. Xu, W. Xiong, K. Ahmad, Electrocoagulation treatment of arsenic in wastewaters: a comprehensive review, Chem. Eng. J. 317 (2017) 707–725.
[6] M. Cheng, G. Zeng, D. Huang, C. Lai, P. Xu, C. Zhang, Y. Liu, Hydroxyl radicals based advanced oxidation processes (AOPs) for remediation of soils contaminated with organic compounds: a review, Chem. Eng. J. 284 (2016) 582–598.
[7] Y. Cheng, H. He, C. Yang, G. Zeng, X. Li, H. Chen, G. Yu, Challenges and solutions for biofiltration of hydrophobic volatile organic compounds, Biotechnol. Adv. 34 (2016) 1091–1102.
[8] R. Xu, Z.-H. Yang, Y. Zheng, J.-B. Liu, W.-P. Xiong, Y.-R. Zhang, Y. Lu, W.-J. Xue, C.-Z. Fan, Organic loading rate and hydraulic retention time shape distinct ecological networks of anaerobic digestion related microbiome, Bioresour. Technol. 262 (2018) 184–193.
[9] S.-F. Pan, M.-P. Zhu, J.P. Chen, Z.-H. Yuan, L.-B. Zhong, Y.-M. Zheng, Separation of tetracycline from wastewater using forward osmosis process with thin film composite membrane – implications for antibiotics recovery, Separ. Purif. Technol. 153 (2015) 76–83.
[10] C.D. Adams, J.J. Kuzhikannil, Effects of UV/H2O2 preoxidation on the aerobic biodegradability of quaternary amine surfactants, Water Res. 34 (2000) 668–672.
[11] K. Lutchmiah, A.R.D. Verliefde, K. Roest, L.C. Rietveld, E.R. Cornelissen, Forward osmosis for application in wastewater treatment: a review, Water Res. 58 (2014) 179–197.
[12] W. Xiong, J. Tong, Z. Yang, G. Zeng, Y. Zhou, D. Wang, P. Song, R. Xu, C. Zhang, M. Cheng, Adsorption of phosphate from aqueous solution using iron-zirconium modified activated carbon nanofiber: performance and mechanism, J. Colloid Interface Sci. 493 (2017) 17–23.
[13] X. Li, S. Chen, X. Fan, X. Quan, F. Tan, Y. Zhang, J. Gao, Adsorption of ciprofloxacin, bisphenol and 2-chlorophenol on electrospun carbon nanofibers: in comparison with powder activated carbon, J. Colloid Interface Sci. 447 (2015) 120–127.
[14] W. Xiong, G. Zeng, Z. Yang, Y. Zhou, C. Zhang, M. Cheng, Y. Liu, L. Hu, J. Wan, C. Zhou, R. Xu, X. Li, Adsorption of tetracycline antibiotics from aqueous solutions on nanocomposite multi-walled carbon nanotube functionalized MIL-53 (Fe) as new adsorbent, Sci. Total Environ. 627 (2018) 235–244.
[15] H. Chen, B. Gao, H. Li, Removal of sulfamethoxazole and ciprofloxacin from

aqueous solutions by graphene oxide, J. Hazard Mater. 282 (2015) 201–207.
[16] W. Xiong, Z. Zeng, X. Li, G. Zeng, R. Xiao, Z. Yang, Y. Zhou, C. Zhang, M. Cheng, L. Hu, C. Zhou, L. Qin, R. Xu, Y. Zhang, Multi-walled carbon nanotube/amino-functionalized MIL-53(Fe) composites: remarkable adsorptive removal of antibiotics from aqueous solutions, Chemosphere 210 (2018) 1061–1069.
[17] W. Xiong, Z. Zeng, X. Li, G. Zeng, R. Xiao, Z. Yang, H. Xu, H. Chen, J. Cao, C. Zhou, L. Qin, Ni-doped MIL-53(Fe) nanoparticles for optimized doxycycline removal by using response surface methodology from aqueous solution, Chemosphere 232 (2019) 186–194.
[18] E.M. Dias, C. Petit, Towards the use of metal–organic frameworks for water reuse: a review of the recent advances in the field of organic pollutants removal and degradation and the next steps in the field, J. Mater. Chem. 3 (2015) 22484–22506.
[19] J. Cao, Z.-h. Yang, W.-p. Xiong, Y.-y. Zhou, Y.-r. Peng, X. Li, C.-y. Zhou, R. Xu, Y.-r. Zhang, One-step synthesis of Co-doped UiO-66 nanoparticle with enhanced removal efficiency of tetracycline: simultaneous adsorption and photocatalysis, Chem. Eng. J. 353 (2018) 126–137.
[20] H. Zubair, J. Sung Hwa, Removal of hazardous organics from water using metal-organic frameworks (MOFs): plausible mechanisms for selective adsorptions, J. Hazard Mater. 283 (2015) 329–339.
[21] J.-M. Yang, R.-J. Ying, C.-X. Han, Q.-T. Hu, H.-M. Xu, J.-H. Li, Q. Wang, W. Zhang, Adsorptive removal of organic dyes from aqueous solution by a Zr-based metal-organic framework: effects of Ce(iii) doping, Dalton Trans. 47 (2018) 3913–3920.
[22] Y. Yue, Z.A. Qiao, P.F. Fulvio, A.J. Binder, C. Tian, J. Chen, K.M. Nelson, X. Zhu, S. Dai, Template-free synthesis of hierarchical porous metal–organic frameworks, J. Am. Chem. Soc. 135 (2013) 9572–9575.
[23] R. Abazari, A.R. Mahjoub, J. Shariati, Synthesis of a nanostructured pillar MOF with high adsorption capacity towards antibiotics pollutants from aqueous solution, J. Hazard Mater. 366 (2019) 439–451.
[24] J. Jin, Z. Yang, W. Xiong, Y. Zhou, R. Xu, Y. Zhang, J. Cao, X. Li, C. Zhou, Cu and Co nanoparticles co-doped MIL-101 as a novel adsorbent for efficient removal of tetracycline from aqueous solutions, Sci. Total Environ. 650 (2018) 408–418.
[25] S.Q. Li, X.D. Zhang, Y.M. Huang, Zeolitic imidazolate framework-8 derived nanoporous carbon as an effective and recyclable adsorbent for removal of ciprofloxacin antibiotics from water, J. Hazard Mater. 321 (2017) 711–719.
[26] M.R. Azhar, H.R. Abid, H.Q. Sun, V. Periasamy, M.O. Tade, S.B. Wang, Excellent performance of copper based metal organic framework in adsorptive removal of toxic sulfonamide antibiotics from wastewater, J. Colloid Interface Sci. 478 (2016) 344–352.
[27] L. Xie, Z. Yang, W. Xiong, Y. Zhou, J. Cao, Y. Peng, X. Li, C. Zhou, R. Xu, Y. Zhang, Construction of MIL-53(Fe) metal-organic framework modified by silver phosphate nanoparticles as a novel Z-scheme photocatalyst: visible-light photocatalytic performance and mechanism investigation, Appl. Surf. Sci. 465 (2019) 103–115.
[28] W. C, L. X, K.D. N, C. JP, L. K, Applications of water stable metal-organic frameworks, Chem. Soc. Rev. 45 (2016) 5107.
[29] B.N. Bhadra, I. Ahmed, S.H. Jhung, Remarkable adsorbent for phenol removal from fuel: functionalized metal–organic framework, Fuel 174 (2016) 43–48.
[30] S. Li, T. Wang, H. Zhang, K. Chang, X. Meng, H. Liu, J. Ye, An amine-functionalized iron(III) metal–organic framework as efficient visible-light photocatalyst for Cr(VI) reduction, Advanced Science 2 (2015).
[31] Y. Gao, S. Li, Y. Li, L. Yao, H. Zhang, Accelerated photocatalytic degradation of organic pollutant over metal-organic framework MIL-53(Fe) under visible LED light mediated by persulfate, Appl. Catal. B Environ. 202 (2017) 165–174.
[32] L. Wu, M. Xue, S.L. Qiu, G. Chaplais, A. Simon-Masseron, J. Patarin, Amino-modified MIL-68(In) with enhanced hydrogen and carbon dioxide sorption enthalpy, Microporous Mesoporous Mater. 157 (2012) 75–81.
[33] S. Lijuan, L. Ruowen, L. Mingbu, J. Fenfen, W. Ling, Electronic effects of ligand substitution on metal-organic framework photocatalysts: the case study of UiO-66, Physical Chemistry Chemical Physics Pccp 17 (2015) 117.
[34] H. Niki, P.D. Maker, C.M. Savage, L.P. Breitenbach, An FTIR study of the kinetics and mechanism for the chlorine- and bromine-atomic-initiated oxidation of silane, Chemischer Informationsdienst 16 (1985) 1752–1755.
[35] L. Ai, L. Li, C. Zhang, J. Fu, J. Jiang, MIL-53(Fe): a metal–organic framework with intrinsic peroxidase-like catalytic activity for colorimetric biosensing, Chem. Eur J. 19 (2013) 15105–15108.
[36] S.J. Yang, J.Y. Choi, H.K. Chae, J.H. Cho, K.S. Nahm, R.P. Chong, Preparation and enhanced hydrostability and hydrogen storage capacity of CNT@MOF-5 hybrid composite, Chem. Mater. 21 (2009) 1893.
[37] J.Y. Song, S.H. Jhung, Adsorption of pharmaceuticals and personal care products over metal-organic frameworks functionalized with hydroxyl groups: quantitative analyses of H-bonding in adsorption, Chem. Eng. J. 322 (2017) 366–374.
[38] X. Zhao, D. Liu, H. Huang, W. Zhang, Q. Yang, C. Zhong, The stability and defluoridation performance of MOFs in fluoride solutions, Microporous Mesoporous Mater. 185 (2014) 72–78.
[39] Y. Liu, Is the free energy change of adsorption correctly calculated? J. Chem. Eng. Data 54 (2009) 1981–1985.
[40] M. Kara, H. Yuzer, E. Sabah, M.S. Celik, Adsorption of cobalt from aqueous solutions onto sepiolite, Water Res. 37 (2003) 224–232.
[41] M. Oveisi, M.A. Asli, N.M. Mahmoodi, MIL-Ti metal-organic frameworks (MOFs) nanomaterials as superior adsorbents: synthesis and ultrasound-aided dye adsorption from multicomponent wastewater systems, J. Hazard Mater. 347 (2017) 123.
[42] J.R. Pils, D.A. Laird, Sorption of tetracycline and chlortetracycline on K- and Ca-saturated soil clays, humic substances, and clay-humic complexes, Environ. Sci. Technol. 41 (2007) 1928.
[43] A. Schierz, H. Zaenker, Aqueous suspensions of carbon nanotubes: surface oxidation, colloidal stability and uranium sorption, Environ. Pollut. 157 (2009) 1088–1094.
[44] P. Kulshrestha, G.R. Jr, D.S. Aga, Investigating the molecular interactions of oxytetracycline in clay and organic matter: insights on factors affecting its mobility in soil, Environ. Sci. Technol. 38 (2004) 4097–4105.
[45] X. Wang, J. Lu, B. Xing, Sorption of organic contaminants by carbon nanotubes: influence of adsorbed organic matter, Environ. Sci. Technol. 42 (2008) 3207–3212.
[46] T. Wu, Q. Xue, F. Liu, J. Zhang, C. Zhou, J. Cao, H. Chen, Mechanistic insight into interactions between tetracycline and two iron oxide minerals with different crystal structures, Chem. Eng. J. 366 (2019) 577–586.
[47] D. Yu, M. Wu, Q. Hu, L. Wang, C. Lv, L. Zhang, Iron-based metal-organic frameworks as novel platforms for catalytic ozonation of organic pollutant: efficiency and mechanism, J. Hazard Mater. 367 (2019) 456–464.
[48] N.A. Ramsahye, T. Thuy Khuong, S. Bourrelly, Q. Yang, T. Devic, G. Maurin, P. Horcajada, P.L. Llewellyn, P. Yot, C. Serre, Y. Filinchuk, F. Fajula, G. Ferey, P. Trens, Influence of the organic ligand functionalization on the breathing of the porous iron terephthalate metal organic framework type material upon hydrocarbon adsorption, J. Phys. Chem. C 115 (2011) 18683–18695.